Journal of Fluorescence, Vol. 12, No. 1, March 2002 (© 2002)

Fluorescence Polarization as a Functional Parameter in Monitoring Living Cells: Theory and Practice

Mordechai Deutsch,[1,2] Reuven Tirosh,[1] Menachem Kaufman,[1] Naomi Zurgil,[1] and Arye Weinreb

Received September 7, 2001; revised January 2, 2002; accepted January 2, 2002

The use of fluorescence polarization as a functional parameter in monitoring cellular activation calls for the reliable and accurate measurement of the fluorescence intensity and polarization (FI and FP) of microscopic objects. The relevant experimental parameters that enter such measurements are thoroughly discussed. The possibility of executing FP measurements properly by flow-through systems is compared with that of static cytometry. Remarks on the effects of high-power excitation on markers and cells conclude the paper.

KEY WORDS: Fluorescence; polarization; flow cytometry; static cytometry; excitation power density; photodamage; photo biostimulation; individual living cells.

INTRODUCTION

Fluorescent polarization (FP) is considered to be the first cellular functional parameter [1]. This article deals with the goal of obtaining correct and accurate measurements of minute changes in FP of microscopic fluorescent samples in general and in fluorescent living cells ($\sim 10^{-12}$ litter), as a functional cytometric parameter, in particular.

Thus, in addition to optospectroscopical requirements (note that the arguments and calculations dealt with in this article concerning optospectrospy are of general validity), biological limitations should be considered as well, to prevent interference in the measuring procedures of the investigated live cell functionalty. Practically, this dictates the use of minimum illumination intensity and dye concentration.

There are many reasons for routinely utilizing FP measurement in cytometry. Unfortunately, most cytometrists ignore FP measurement and concentrate solely on measurements of color and intensity, despite the fact that the latter is FP dependent.

In short, transmembrane stimulation of lymphocytes, at the G_0-G_1 resting phase, induced by specific antigens, mitogens, or antibodies to certain cell-surface molecules, results in a complex series of well-characterized molecular events, culminating in lymphocyte activation, transformation, mitosis, and finally apoptosis [2–4]. These events are associated with early changes in membrane potential coupled with an influx of Na^+ and changes in pH, followed by the influx and internal release of Ca^{2+} ions. In the course of cell activation the processes linking early and late intracellular events involve conformational changes of cytosolic enzymes and/or their regulatory proteins, as well as their intracellular matrix reorganization [5–7]. Monitoring these early structural changes is done by measuring the FP of intracellular fluorescent probes, a measure that was utilized for monitoring different cellular events [8,9–11].

FP measurements of cellular fluorescent markers, mostly of fluorescein, were carried out in two ways:

(1) Cell suspensions in a cuvette [12–14,15–22] and
(2) Flow cytometry (FC) [23–35].

[1] The Biophysical Interdisciplinary Center for the Research and Technology of the Cellome, and The Jerome Schottenstein Center for Early Detection of Cancer, Bar-Ilan University Ramat-Gan, Israel 52900.
[2] To whom correspondence should be addressed. Tel: 927-3-534-4675, 972-3-531-8349; Fax: 972-3-534-2019; email: motti_d@netvision.net.il

1053-0509/02/0300-0025/0 © 2002 Plenum Publishing Corporation

Cuvette measurements have four principal defects: (i) because fluorescence emission is measured simultaneously from many cells, it is not possible to discern any existing heterogeneity within the population; (ii) cuvette measurements offer no opportunity to distinguish between the desired fluorescence emitted from the intracellular dye and the undesired background fluorescence emitted by the dye in the solution; (iii) weaker fluorescing cells are measured with less accuracy than stronger fluorescing cells, because of photon statistics; and (iv) relatively large quantities of cells are required for reasonably accurate measurements. In spite of these defects, meaningful results can still be achieved with this procedure.

In relation to cuvette measurements, it is to be expected that in FC the accuracy and sensitivity of FI measurements would improve because they are made on single cells. However, there are grounds to suspect that FC is significantly affected by anisotropy because most FC utilizes coherent, high-polarized lasers. Hence, scatter, as well as fluorescence signals, are very likely to be anisotropy, a fact that introduces randomness and distortion in FI measurements, as well as dependency on the detectors' location in respect to the excitation beam [36].

Both methods dictate the need for a large number of cells to achieve meaningful statistics and do not enable the tracing of the same individual cells (e.g., before and after stimulation). Such consecutive measurements offer the highest reliability for detecting the effect of cell activation as monitored via changes in FI and/or FP, as well as any other optical parameter, and by definition can be performed only via static cytometry (SC).

In the following section, IFFP measurement, using FC and special in-house designed and constructed SC, will be discussed in general, with specific emphasis on cases in which only low excitation intensities and dye concentrations are available.

THEORY: FACTORS AFFECTING THE ACCURACY OF IFFP MEASUREMENTS

The Influence of the Numerical Aperture on the FP Measurements

Geometry

The ideal geometry for FP measurements requires the macroscopic detection of the vertical and horizontal fluorescence components $I_{\parallel}$ and $I_{\perp}$, correspondingly, in a direction normal to the vertical excitation beam and at a distance far enough from the sample being measured, to ensure collection of only parallel-emitted rays. In such a case, $FP = [I_{\parallel} - I_{\perp}]/[I_{\parallel} + I_{\perp}]$. However, in contrast to the above ideal macroscopic collection arrangement, in a microscopic detection setup for FP measurements (of microscopic samples, both in FC and SC), excitation and fluorescence radiation are collected over a range of angles. To analyze the problem of measuring FP in such a case, consider Fig. 1. A fluorescent molecule rests at the origin (center of a sphere). Its dipole moments for absorption and emission are assumed to be parallel to each other and to the exciting electric field $\mathbf{E_{ex}}$, which is polarized along **Z** and travels in the **X** direction. Its emitted intensity is symmetrical with respect to the dipole axis; its strength is maximal and equal in the equatorial plane (**1** → **2**), decreasing along each longitude (**1** → **3** to zero at the pole (point **3**). From symmetry, this holds true for all eighths of the sphere. For an ensemble of randomly oriented molecules, the absorbing probability distribution is not uniform, resulting in a cone (symmetrically oriented about the **Z** direction) of excited molecules. This distribution is termed photo-selection and is proportional to $\cos^2\theta$, where θ is the angle between the exciting vector field, and the absorbing dipole axis. In such a case, the FP monitored along the equator (**1** → **2**) is equal at all points. However, along the longitude (**1** → **3**), FP gradually decreases to zero at the pole. Thus FP measurements at different latitudes yield a range of FP values.

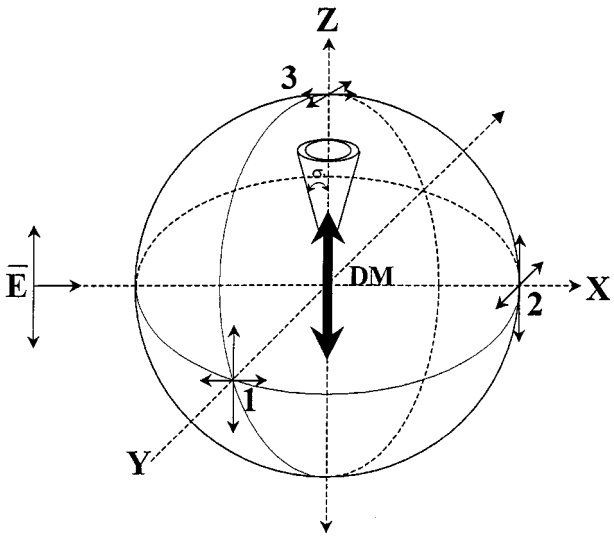

Fig. 1. The field of a radiating dipole. A fluorescent molecule rests at the origin. Its dipole moment (DM) is parallel to the exciting electric field **E**, which is polarized along *z* and travels in the *x* direction. Its emitted intensity is symmetrical with respect to the dipole axis; its strength is maximal and equal in the equatorial plane (1 → 2) decreasing along each longitude (1 → 3) to zero at the pole (point 3). When an ensemble of randomly oriented molecules is present, a cone of excited molecules is obtained.

In a microscope, the objective collects a cone of light defined by its numerical aperture. This cone contains rays crossing different latitudes, thus deforming the true FP. The larger the numerical aperture, the greater the deformation of the measured polarization.

Calculation of the Relative Change of the Measured FP

For accurate monitoring of cell activation when assessing via measurement of the variations in the functional cytometric indicator FP, one should carefully examine the influence of the numerical aperture (NA) upon $\Delta P/P$, the relative measured change in FP taking place in an individual cell after biological stimulation or other manipulation. For convenience, as well as for clarifying the source of that question, Appendix A presents the calculation of FP as a function of the NA, a dilemma that was previously examined by various approaches [29,37]

To evaluate the angular dependence of the measured FP, see Fig. 2. A flourescent sample is placed at point **0**, the origin. The coordinate system **XYZ** fits an ideal FP measurement in which the exciting beam $\mathbf{E_{ex}}$ is polarized in the **Z** direction and propagates along **X**, while the emitted beam is measured as it propagates along **Y**. The coordinate system **xyz** relates to a non-ideal measurement in which rays of fluorescent radiation, which deviate from the **Y**-direction, are also collected. The FP of such a beam, for which the marginal ray subtends the **XY** plane by an angle $\boldsymbol{\theta}$ and has an azimuthal angle $\boldsymbol{\phi}$ from the **Y** direction, is calculated in Appendix A, where, for brevity, the letter *P* is sometimes used instead of *FP*. The measured

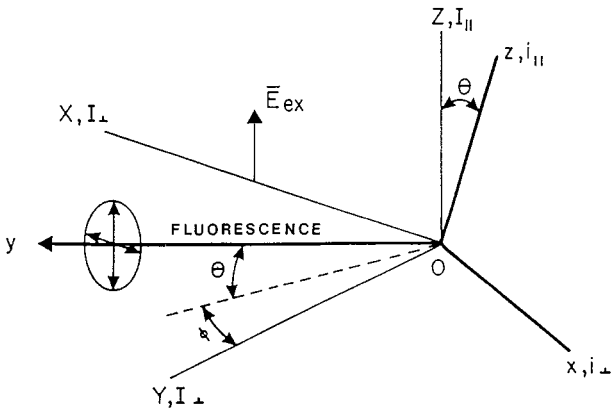

Fig. 2. Axis system for standard (**XYZ**) and non-ideal (**xyz**) polarization measurement. The exciting beam polarized along **Z** propogates along **X**, and the emitted beam propagating along **Y** is measured. The coordinate system **xyz** relates to a non-ideal measurement in which rays of fluorescent radiation are collected, even though they deviate from the **Y**-direction to a maximum angle of Θ and Φ along θ and ϕ, respectively.

P is the summation of all rays emitted into the solid aperture angle, defined by Θ and Φ:

$$P(\Theta, \Phi) = \frac{\Sigma\, i_{\parallel}(\theta, \phi) - \Sigma\, i_{\perp}(\theta, \phi)}{\Sigma\, i_{\parallel}(\theta, \phi) + \Sigma\, i_{\perp}(\theta, \phi)} \tag{1}$$

Integration over θ and ϕ gives:

$$\frac{1}{P(X)} = \frac{2}{P\left[1 + \left(\frac{\sin X}{Y}\right)\right]} - \frac{1 - \left(\frac{\sin X}{X}\right)}{1 + \left(\frac{\sin X}{X}\right)} = \frac{a}{P} - b \tag{2}$$

where $P(X)$ is the measured value of the polarization, which depends on both the true polarization P and the angular aperture X. When $X = 2\theta = 2\phi = 0$, then the measured polarization is the true value P. Note that P(X) is not corrected for the collection of the excitation beam from various angles, which is a source of deviation from P. The justification for not taking these deviations into account is that, for the static cytometer (SC) used in this study, the radius of the exciting beam is less than 1% of the radius of the objective lens, before impinging on it. Therefore, the impinging beam remains narrow and axial when illuminating the entire cell.

For small values of X, the measured value P*(X) approximates P(X) but, unlike P(X), has a value directly proportional to the true value P, as given in Eq. (3):

$$P^*(X) = \left(\frac{P}{2}\right)\left[1 + \left(\frac{\sin X}{X}\right)\right] = \frac{P}{a} \tag{3}$$

For any given aperture X, the correction factor to convert P*(X) to the true value P is given by $M = 2/[1 + (\sin X/X)]$, which is independent of P.

Actually, the quantity of interest, $\Delta P/P$, is the relative change in the true P after any biological manipulation. In Eq. 2, it is easily shown that $\Delta P/P$ is related to $\Delta P(X)/P(X)$, the relative change in the measured P(X), by:

$$\frac{\Delta P}{P} = \left[\frac{\Delta P(X)}{P(X)}\right]\left[1 - \frac{Pb}{a}\right]$$

where *b* and *a* are defined in Eq. (2) above. Thus the percentage change in the true polarization depends not only on the percentage change in the measured polarization but also on the true polarization itself. In practice, this means that the same measured relative change $\Delta P(X)/P(X)$, after biological manipulations, yields different $\Delta P/P$ values, depending on the true P values, which are not known. Thus the real contribution of

biological stimulation to the FP cannot be estimated accurately.

By contrast, it is readily shown that, when Eq. (3) holds, the following relation is true,

$$\frac{\Delta P}{P} = \frac{\Delta P^*(X)}{P^*(X)}$$

which means that the percentage change in the true polarization is identical to the percentage change in the measured polarization. This property makes it of great practical value to work in the range of small X to enable the accurate determination of the change in polarization resulting from biological stimulation.

Accuracy of a Polarization Measurement

The number of events, N, which are monitored, are usually composed of two parts, the true fluorescence, N_f, and the background, N_b, which may have several contributions (e.g., dark current, autofluorescence of the biological material, Rayleigh and Raman radiation, and emission from leaked marker molecules). As the ratio of N_f/N_b decreases, the measurement dispersion increases.

The relationship between the required number of photoelectrons (N_{pe}) and a given coefficient of variance (CV) (CV = dP/P) of the polarization results, is derived in Appendix B.

$$N_{pe} = \left[\left(\frac{1 - P^2}{P}\right) 1 \Big/ \frac{dP}{P}\right]^2 \qquad (4)$$

Therefore the accuracy of a polarization measurement depends not only on the number of photons counted (from elementary, statistical considerations) but also on the degree of the polarization itself. In Eq. (4) we see that, to obtain a CV of 3% for a polarization of 0.2, about 25,600 photoelectrons are needed.

Absorption of the Exciting Beam by the Cell

The cross section of a TEM_{00} laser beam gives a Gaussian distribution of the intensity around its center of the form $i(r) = i_0 \exp(-2r^2/\omega^2)$, where *r* is the radial distance from the center of the beam and ω is the distance from the center at which the intensity decreases to $1/e^2$ of its maximum intensity i_0 at the center of the beam. In the calculation of the absorption of the exciting light by the fluorescent marker, homogenously spread over the cell volume, each cylindrical optical path within the cell has a different incident intensity depending on the distance of this path from the center of the exciting beam. Assume a beam of effective width of the size of the cell (i.e., ω is equal to the radius of the cell) and the cell centered to the beam center. In this case, the calculation, derived in Appendix C, gives an absorption (A)

$$A = I_0\, 2.3\varepsilon c(2R)\left(1 + e^{-2}\int_1^0 e^{2x^2}\,dx\right)$$

$$= I_0\, 2.3\varepsilon c(2R)0.68$$

where I_0 is the overall intensity of the exciting beam, ε the molar decadic absorption coefficient of the dye, *c* its concentration in the cell, and *R* the radius of the cell.

In a case in which the cell and the beam center do not coincide, or the dye density varies intracellularly, then a different approach should be taken, as further explained in Appendix C.

MATERIALS AND METHODS

Preview

Most, if not all studies of living cells based on FP measurements with cuvette, flow, or static cytometers, were initiated by the promising but problematic approach to a cancer immunodiagnosis test, named the Structuredness of Cytoplasmic Matrix, or SCM, test [8,14]. In this test, fluorescein is introduced into the cell via enzymatic hydrolysis of FDA [38], and the functional parameter, Intracellular Fluorescein Fluorescence Polarization (IFFP), is measured. In the following, Cercek's procedure will be followed as a method reference.

In a hetrogenious media such as intracellular media, the same type of dye may be hosted by different intracellular zones, which may possess different physiochemical features. Thus dissimilar influences upon the spectoscopic host fluorescent molecule are induced, and the total cell FP is an intensity-weighted average measure that may be wavelength (excitation/emmision) dependent. In such a case the best observed changes in cell functionality, measured via FP, may be wavelength (excitation/emmision) dependent as well [39] and thus require selected narrow bandwidth measurements. Still, the quest for high FI generally led researchers to compromise the best spectroscopical condition, which harvests the most significant change in FP as a functional parameter, and to choose the conditions that yielded the maximum quantum efficiency. For example, after biological stimulation, the maximum depolarization observed at 510 ± 5 nm when flourescein in FDA-labeled stimulated cell is exicited at 470 ± 10 nm [8]. In spite of this fact the excitation wavelength was raised to 490 nm [40], at which the absorption of

fluorescein is the strongest, and a broader emission band and longer wavelengths were used. Hocking, *et al.* [16] and Rolland, *et al.* [40] obtained, after stimulation, a fluorescence depolarization of 10–20% in cuvette measurements. When they shifted to FC, where 488-nm argon line was used, this change went down to 2.8 ± 1.1%, with a CV of 2% [23,34].

The Use of Flow Cytometry in FP Measurements

Excitation

Almost all researchers have used a 5-W (all lines) argon laser (Spectra Physics or Coherent) as the source of excitation. The excitation wavelength in most of these investigations was 488 nm, with an intensity at the interrogation point of hundreds of milliwatts up to 1 W. An exception to this are the earlier works of Beisker *et al.* [41–43] who used a 10-mW He-Cd laser with an effective spot intensity of 5 mW.

Emission

In most of the investigations the fluorescent emission was measured either through a long-wavelength cut-off filter ($\lambda > 500$ nm) or a broadband interference filter (500–560 nm) to collect most of the fluorescein emission.

Dye Concentration

The lower the dye concentration, the deeper the FP change is. For IFFP measurements [8], cells were exposed to 0.6 μM FDA in phosphate buffer saline (PBS) coloring solution, for approximately 4 minutes at 27°C.

Again, the quest for high fluorescence intensity (FI) caused the elevation of dye concentration 10fold, 100-fold [25], or even 400-fold [33], as well as a raise in the coloring temperature. Several groups [19,34], reported on the influence of the dye concentration on the measured IFFP.

In general, reduction of dye concentration is recommended because overcoloring may cause morphological changes of the cell [44].

Sampling Time

The velocity of the sample flow is 1–10 m/s. This velocity range is dictated by the necessity for a laminar flow of constant velocity. Assuming a particle size of the order of 6–7 μ, for the average velocity of 5–6 m/s and a commonly used illumination beam that intersects the direction of the flow at a width of 2–6 μm, one obtains a pulse width of 1–2 μsec. Most groups worked under these conditions, realizing that there is not much leeway of choice in these working parameters [45].

Numerical Aperture

The numerical aperture varied between the various groups from 0.25–0.6.

Correlated and Uncorrelated Systems

The correlation between the intensity measurements of the vertically and horizontally polarized emission beam is critical for the accuracy of the degree of FP. The problem of uncorrelated systems has been thoroughly treated by Pinkel, *et al.* [46]. A non-correlation maximum also ruled other systems [28,29,31,33].

The Use of Static Cytometry in FP Measurements

In the present work, the in-house designed and built *Individual Cell Scanner (ICS)* was utilized. The ICS is a multiparametric, computerized, static cytometer. Briefly, this system permits the repetitive spectroscopic measurement of individual cells within a population of many cells, while the location of each cell is preserved during various manipulations of the cells and/or their surrounding medium.

The central feature of the system is a cell tray, which localizes cells in an array of individual cell traps, 20 μm pitched and having an effective opening diameter and height of 6–25 μm (depending on the investigated cell dimension). The cell tray is done via common Microelectromechanical Systems (MEMS) techniques. The cell tray is mounted on a computer-controlled stage that enables repeated scanning of the same cells. The electronic detector operates in a preset photon counting mode, permitting the measurement of low and high FI with the same degree of precision. Basic features of the methodology behind the ICS design were published previously.

Because the measurement is static and the sampling time is not limited, excitation intensities can be very low. Problems relating to mechanical forces, high excitation power density (PD), and/or high dye concentrations are negligible. With ICS the majority of uncorrelated measurement factors are null because most optical trajectories use the same path and optical elements. In addition, the excitation geometry is such that the entrance pinhole, not the exciting beam, is imaged onto the plane of the cells, so that instabilities of the excitation beam will, at most,

cause a change in intensity but not in the location of the excitation spot.

Generally, biological cells are highly structured particles. Light propagated through the cell will necessarily be scattered in all directions with different polarizations, leading to additional depolarization of excitation, as well as of emission. Theoretical and experimental investigations show that the largest deviations from the true FP occur when the angle between the excitation beam and the detection direction is 90°. Substantially smaller differences were found at 0° and 180° [47,48]. This favors a backward fluorescence detector arrangement, known as epi-illumination, in conventional microscopy as is generally used in SC.

RESULTS

The Laser Power Required to Measure FP Accurately

Utilization of IFFP as a functional parameter calls for changes of about 7% in FP, because of stimulation of cells, in order to have meaningfull implication. Relating to this as an opening line for calculation, a CV smaller than 3.5% in FP (or a CV of FI of about 0.7%) measurement is required. Assuming a commonly observed FP of the order of 0.2 (for lower FP values a greater number of photoelectrons is required for the same CV), the required number of photoelectrons, calculated from Eq. (4), is 25,600. Some investigators reported a depolarization of less than 3% as being significant [23,32]. In such cases, a much higher measurement accuracy would, of course, be required.

The different parameters that enter the FP accuracy calculation in both flow-through and static cytometers are discussed in the following.

Flow Versus Static Systems

The different flow systems, as surveyed in the literature, include a variety of elements. This article deals with an average system designed for FP measurements and tries to determine the light attenuation caused by the given elements.

The average photoelectron yield of the photomultipliers used in the wavelength region of the fluorescein fluorescence (500–600 nm) is about 7% [34]. The transmission of the light diffusers and of the long-wavelength cut-off filter (LWCF) is about 80% for each. Usually two excitation lenses were used, each of which reflects about 5%, giving a transmission of $(0.95)^4$. In addition, quarter-wavelength plates, which transmit 85%, were used to permit the change of the plane of polarization of the exciting radiation. On the emitting side, a broadband interference filter (BBIF) was used with a transmission peak at the center of the fluorescence band, or a LWCF. Sometimes both were used, to permit maximum passage of the emitted energy. For the SC used in this study, a narrowband interference filter was used, which transmits about 10% of the emitted fluorescence. The Glan-Thompson polarizer transmits 50% of the light.

For calculation of the light-gathering power in FC, a representative numerical aperture (NA) of 0.4 was chosen, where the aperture angle θ is 23.6° for an air gap. Therefore, the relative angle of the cusp of light collection is $\Omega/4\pi = \sin^2 \theta/2 = \sin^2 (23.6/2) = 0.042$. The choice of NA is limited. Increasing the NA improves light collection, but decreases the depth of focus, and, hence, increases the fluctuations of the measured intensities caused by the uncertainty of the cell trajectory. Likewise, increasing the depth of focus by decreasing the NA decreases fluctuations but also reduces light collection from the cell, and the signal-to-noise ratio is increased (because of the contribution of the collected light from the region around the cells). Moreover, inspection of Eq. (2) shows that for large apertures (large $\mathbf{X}$) the second expression on the right side of the equation is not negligible. Hence, changes of P(x) would not only be dependent on X (which is a system constant) but also on the real polarization P, which depends on the measured sample. This would require a different correction factor for each FP value.

This problem is non-existent in the SC used, because the location of the cell with regard to the exciting radiation is well known and fixed.

To avoid dye concentration depolarization, a solution of 0.6 μM FDA in PBS was used for the SC measurements, which gives an average concentration of intracellular fluorescein of 5×10^{-6} mole/L (see Appendix D).

According to the calculation given in Appendix C, the absorbed radiation A equals:

$$A = I_0\ 2.3\varepsilon c(2R)0.68$$

where I_0 is the intensity of the exciting radiation, ε the decadic molar absorption coefficient (8,320 M^{-1} cm^{-1} at 442 nm), c the concentration of the marker in the cell, and R (assumed to be 3.5 μm) the radius of the cell. The fluorescence quantum yield of fluorescein is assumed to be 0.8 at 442 nm.

The intensity of the exciting radiation I_0, which is needed to obtain a CV of 3% for an FP level of 0.200, results from the product of all the parameters discussed

above. To obtain 25,600 photoelectrons with a photomultiplier of 7% efficiency, 365,700 photons are required.

The following calculation is used to determine I_0, using the above data, which is summarized in Table I.

$$\begin{aligned}365{,}700 \text{ photons} = I_0 &\cdot 0.8 \cdot 0.8 \cdot (0.95)^4 \cdot 0.85 \cdot 0.1 \\ &\cdot 0.5 \cdot 0.042 \cdot 0.8 \cdot 2.3 \cdot 0.68 \\ &\cdot 8320 \cdot 5 \cdot 10^{-6} \cdot 7 \cdot 10^{-4} \\ &\cdot 10^{-6} \text{ sec} = I_0\, 339 \cdot 10^{-16} \text{ sec}\end{aligned}$$

Hence,

$$I_0 = \frac{365{,}700 \cdot 10^{16}}{339} \text{ photons/sec}$$

$$\cong 1.1 \cdot 10^{19} \text{ photons/sec}$$

The energy of an exciting photon at 442 nm (He-Cd 442 nm line yield similar change in FP after stimulation as 470 nm) is $4.47 \cdot 10^{-19}$ J. Therefore, the required intensity of the exciting radiation is

$$1.1 \cdot 10^{19} \cdot 4.47 \cdot 10^{-19} \text{ J/sec} = 4.92 \text{ W}$$

Such single-laser-line power is not commercially available for cytometry, and it would be too high an intensity, causing damage to the cell and its fluorescent marker, a phenomena discussed later.

To obtain the required number of 25,600 photoelectrons for one cell measurement, using weaker lasers, one might consider an increase in the concentration of the dye [25,33], but this would lead to serious problems of concentration depolarization or even to changes in cell morphology [44].

Table I. Use of Numerical Values of the Relevant Magnitudes That Enter the Calculation of the Required Excitation Intensity in Flow Cytometers

Magnitudes	Values
PMT yield	0.07
Transmission of LWPF	0.80
Transmission of light diffusers	0.80
Transmission of four excitation lenses	$(0.95)^4$
Quarter-wavelength plate transmission	0.85
NBIF transmission	0.10
Glan Thompson polarizer transmission	0.50
Light-gathering power	0.042
Fluorescein fluorescence quantum yield	0.80
Intracellular fluorescein concentration	$5 \cdot 10^{-6}$ M
Decadic molar absorption coefficient	8320 M^{-1} cm^{-1}
Cell radius	3.5 μm
Number of emitted photons incident to PMT	365,700 photons
Measurement duration	10^{-6} s

Static Cytometry

Calculation of the Required Excitation Power

The relevant elements and the role they play in FP measurement by the SC system, are now examined.

In SC, the accurate localization of the investigated cell in the interrogation region permits the use of an NA of 0.6. Therefore, for air, the opening angle θ will be 37° and the relative light collection will be 0.1.

The glass illuminator (two reflecting surfaces) in the ICS has a transmission $(0.95)^2$. The use of a plane glass reflector was preferred to the use of a dichroic mirror, which is usually employed in epifluorescence systems, because the latter was found to strongly influence the polarization properties of the emitted radiation.

The transmission of the Glan-Thompson polarizing prism is 0.5. The transmission of the narrowband interference filter is approximately 0.10.

The quantum yield of the fluorescence is again assumed to be 0.8, and that of the multipliers used in this research is 0.18. The absorbed part of the radiation by the cell is like that calculated above (Appendix C). Therefore:

$$\begin{aligned}I_{AB} &= 0.68 I_0 \varepsilon c(2R) \cdot 2.3 \\ &= 0.68 \cdot I_0 \cdot 8320 M^{-1}\, cm^{-1} \\ &\quad \cdot 5 \cdot 10^{-6} \text{ M} \cdot 7 \cdot 10^{-4} \text{ cm} \cdot 2.3 \\ &= 0.45 \cdot 10^{-4}\, I_0\end{aligned}$$

The characteristic measuring time of one cell is in the range of 5–70 ms or by large, less than 0.1 sec. Hence, to obtain 25,600 photoelectrons:

$$\begin{aligned}25{,}600 \text{ photoelectrons} = I_0 &\cdot 0.1 \cdot (0.95)^2 \cdot 0.5 \cdot 0.1 \\ &\cdot 0.8 \cdot 0.18 \cdot 0.45 \cdot 10^{-4} \\ &\cdot 0.1 \text{ sec} \\ &= I_0 \cdot 2.92 \cdot 10^{-9} \text{ sec}\end{aligned}$$

giving:

$$I_0 = 8.8 \cdot 10^{12} \text{ photons/sec}$$

and for an exciting photon of 442 nm, a power of:

$$8.8 \cdot 10^{12} \cdot 4.47 \cdot 10^{-19} \text{ J sec}^{-1} \approx 3.9\ \mu\text{W}$$

is obtained.

The above calculations are presented, not so much to obtain absolute values for the relevant parameters, but rather to exemplify the difference between the illumination conditions in FC versus those used here (mainly

because of their typical measurement duration), amounting to about six orders of magnitude.

Practically, to obtain such small excitation energies (of a few microwatts) from commercially available lasers (tens or hundreds of milliwatts to a few watts), a combination of pinholes (of 25, 50, and 100 μ) and density filters are used (see Appendix E).

Interfering Signals

Intensity Discrimination Capabilities

- *Dark current*: Dark current is measured before the fluorescence measurements and deducted from the measured intensity per cell. For the Hamamatsu R647 photomultiplier (PMT), it is typically 80 counts/sec. For a preset count of N = 30,000, counted within 0.1 sec, the integrated dark current will be 8/30,000 ≅ 0.02% of the signal.
- *Scattering intensity*: For an excitation power of 4 μw, the scatter is ~100 Hz, which constitutes about 10/30,000 = 0.03% of the signal. These background intensities, even if not deducted from the total intensity signal, would be insignificant.
- *Autofluorescence*: The ability to monitor and eliminate autofluorescence by the SC is demonstrated by the following experiment, as illustrated in (Fig. 5). An empty cell tray was scanned, yielding a background signal of approximately 0.1 KHz. The carrier was then loaded with human living lymphocytes and rescanned, yielding the locations of two cell subgroups having intensities of ~0.1 KHz and ~0.47 KHz. The loaded cell tray was then exposed for 2 minutes to the staining solution of PBS and FDA and rescanned.

  The results show that the 0.47-KHz group of the second scan were stained to give an average of ~37 KHz and those of ~0.1 KHz gave ~0.4 KHz (caused by IF leakage).

  The capability of measuring different background contributions on an individual cell basis, before staining, offers a unique way that might permit pure measurement of N_f.
- *Long integration time*: Using continuous excitation light sources, the integration time (long or short) is relevant only if the background is measured when the signal measurement is not on (i.e., when the integration time precedes or follows the duration of the signal pulse). In contrast to flow cytometers, this possibility cannot occur in static cytometers, where the location of cells is predetermined, because the noise is measured only when the signal is measured (i.e., after cell positioning in the interrogation region). Therefore the signal-to-noise ratio is constant for a given N_f.

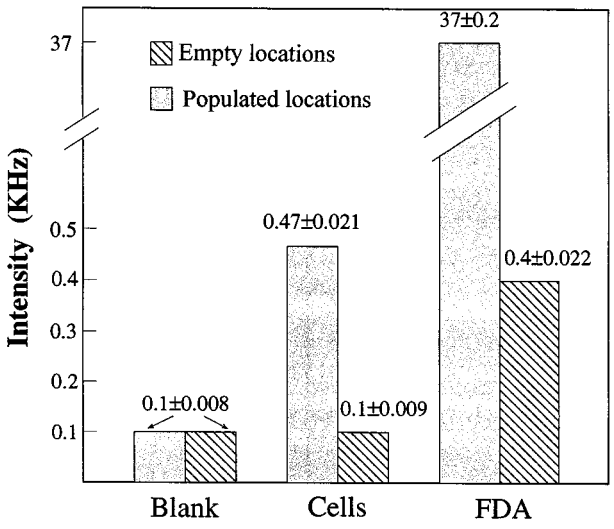

Fig. 3. Average intensity measurements of empty (▨), and populated (□) locations. Following exposure of the cell tray to FDA-PBS staining solution, the intensity of those populated locations having intensity of ~0.47 KHz before staining, increased to ~37 KHz. Blank stands for unloaded cell tray measurements.

Polarization Discrimination Capabilities

Fluorescence background resulting from unbound markers, as well as autofluorescence, can be eliminated when using static cytometers. An example illustrating this capability is shown in Fig. 6, where cell-ligand interaction intensity FI versus FP is displayed on a series of panels, demonstrating the staining and washing of a murine B cell hybridoma cell with fluorescein isothiocyanate (FITC)-conjugated goat anti-mouse F(ab)′₂.

Cell staining and washing of unbound reagent is performed while the cells are resting in the cell tray. This method is quick, easy to perform, does not cause significant loss of cells or viability and can be applied to extremely small cell samples. First, FI and FP of the unbound antibody was measured (see Fig. 6, panel 1). Then the autofluorescence intensity and polarization of unstained cells were determined (see Fig. 6, panel 2). The cells were then exposed to the FITC-conjugated antibody, and FI and FP were determined just before rinsing the unbound conjugated antibody (see Fig. 6, panel 3). Finally, excess (unbound) fluorescent marker was removed by rinsing, leaving behind only the stained cells, and FI and FP were remeasured (see Fig. 6, panel 4).

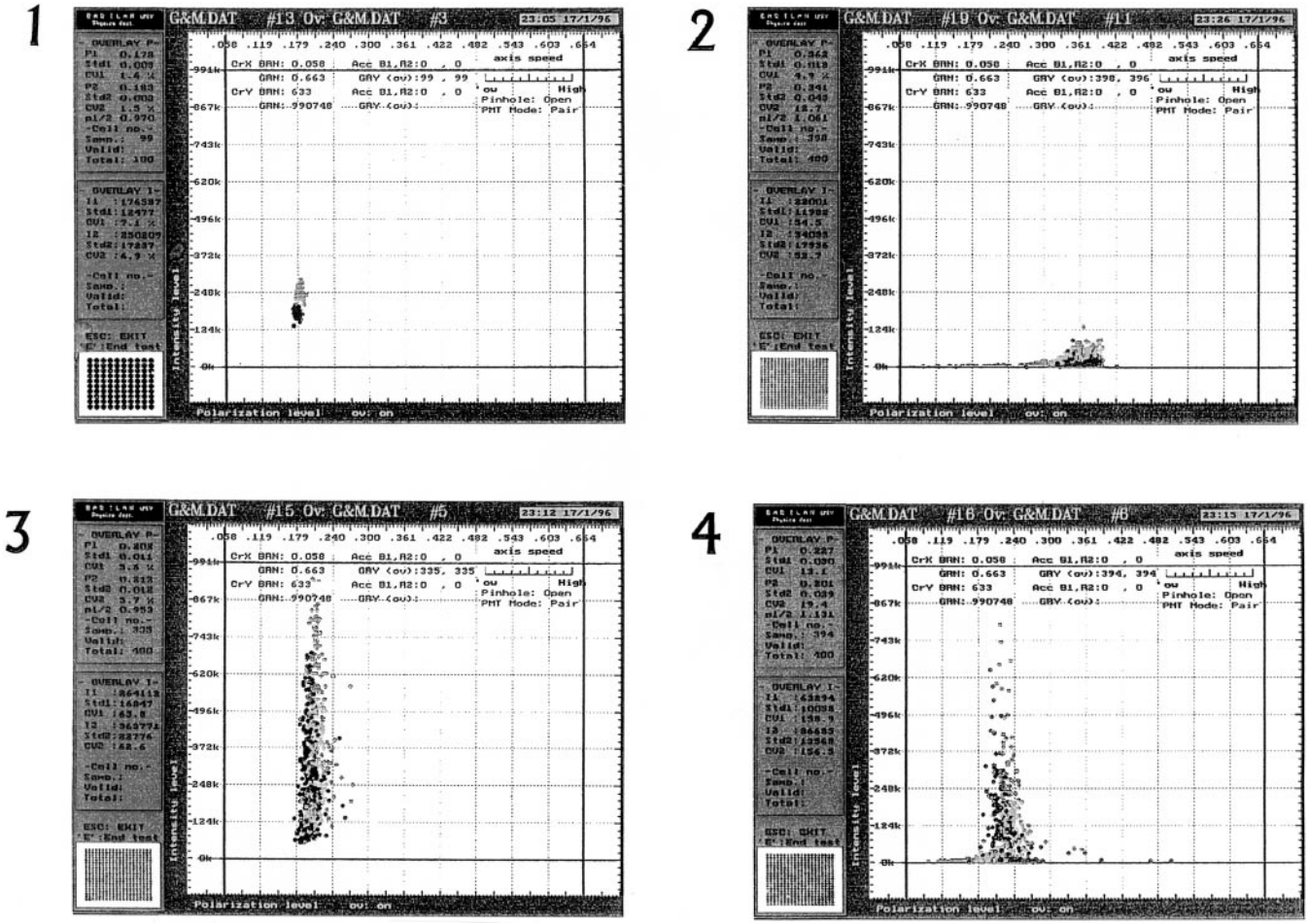

Fig. 4. Scatter grams of fluorescence intensity (FI) (ordinate) versus fluorescence polarization (FP) (abscissa) of surface marker of mouse B cell hybridoma cells monitored by the ICS. Panel 1: suspension of FITC-conjugated antibody. Panel 2: unstained cells. Panel 3: FITC-labeled cells just before rinsing of unbound marker. Panel 4: FITC-labeled cells after rinsing of unbound marker.

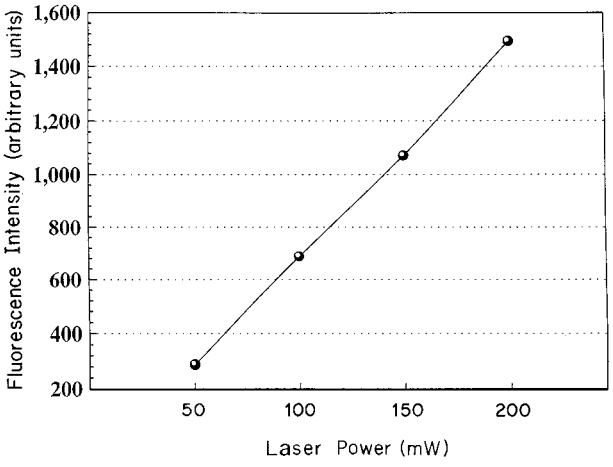

Fig. 5. FI of beads as a function of argon laser (472 nm) power between 50 and 200 mW. CV did not exceed 1%.

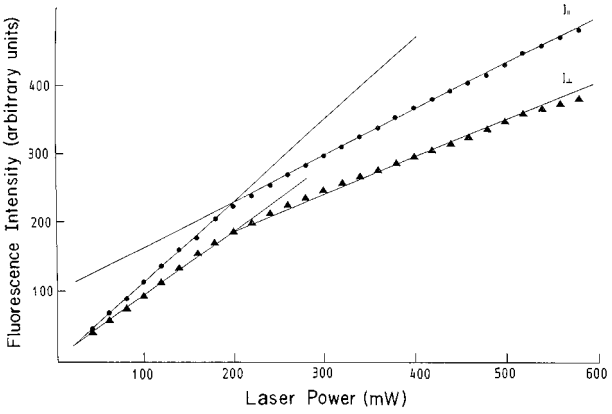

Fig. 6. Normal (▲) and parallel (●) FI components of fluorescein (5 μM) in a glycerin-water mixture (4:1) as a function of argon laser (472 nm) power between 0 and 600 mW. The break of the curves at around 200 mW is purely incidental. In both segments of both lines, the behavior of the measured intensity was linear with the laser output.

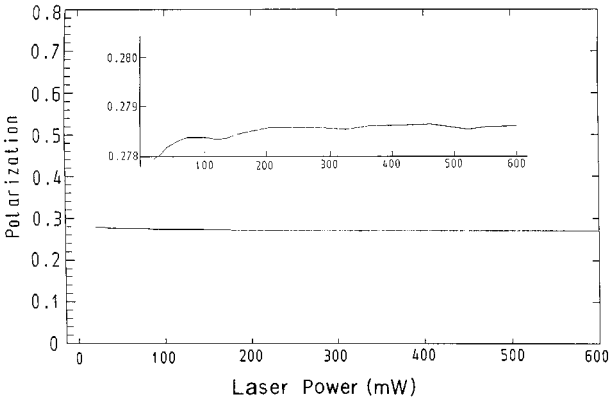

Fig. 7. Polarization of fluorescein (5 μM) in a glycerin-water mixture (4:1) as a function of laser power between 0 and 600 mW. The curve in the insert is a magnification of the figure. The polarizations stay practically constant for all intensities.

The autofluorescence had the lowest FI, coupled with the highest FP level, and the unbound fluorescent marker in solution exhibited the lowest FP level (0.179). As expected, the FP of the stained cells in the presence of the unbound probe was lower than after rinsing. The same approach was also successfully used to monitor indirect staining (unpublished data).

Photobleaching

Linearity tests performed on fluorescent beads (6.5 μm diameter, Polyscience, Inc., Warrington, PA, USA) (Fig. 7) and fluorescein solution in a mixture of 4:1 glycerin-water (Fig. 8) show no trace of photobleaching in the laser range (488 nm, all lines 5W, Spectra Physics) of excitation, 50 to 600 mW. (The breaks in the line in Fig. 8 at about 200 mW are attributed to a change in the laser beam cross section. Note that both segments of both lines are still linear). The FP of 4:1 glycerin-water mixture

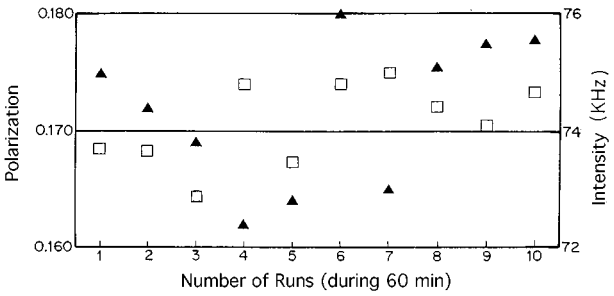

Fig. 8. FI (□) and FP (▲) obtained on one individual cell during 10 scans of 10 × 10 field. The time interval between two sequential measurements is 6 minutes. FI = 74.14 ± 0.68 KHz (CV = 0.92%), FP = 0.172 ± 0.006 (CV = 3.6%).

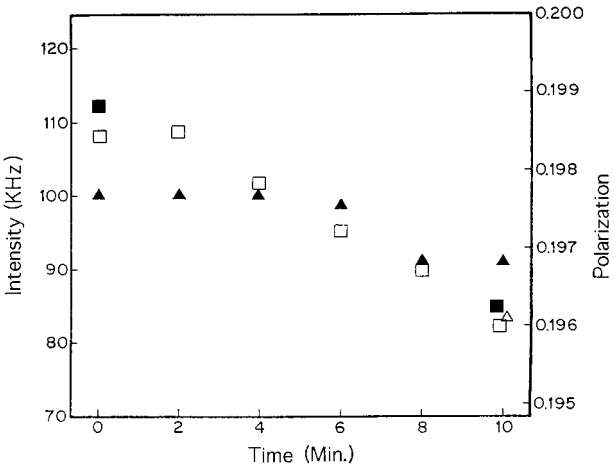

Fig. 9. Direct examination of fading. Average FI (□) and FP (▲) obtained in 10 sequential scans. For control measurements, two other cell trays were treated identically. One of them (■) was scanned only twice, at time points 0 and 10, and the other (△) only once, at time point 10. (For detailed explanation see text.)

also remained constant throughout the excitation range (Fig. 9).

Photobleaching effects were examined on individual cells under regular IFFP measurement conditions [49]. A field of 10 × 10 stained cells was scanned repeatedly (10 times at 6–7-minute intervals). The measured cells were continuously rinsed during measurement with FDA-PBS staining solution to simultaneously compensate for intracellular fluorescein efflux and eliminate fluorescent background signals. Figure 10 shows ten successive measurements for FI and FP of one individual cell (with average values of 74.145 ± 0.68 KHz (CV = 0.92%) and 0.172 ± 0.062 (CV = 3.6%), respectively).

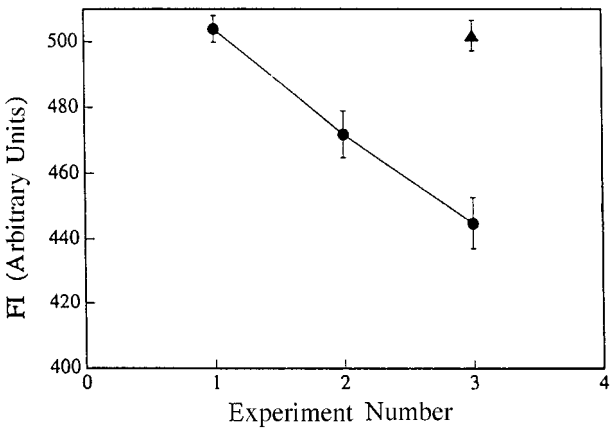

Fig. 10. Three repetitive runs on the same fluorescent beads performed on FACSort, ●, illuminated in each of the 3 runs; ▲, illuminated only on the fourth run.

Direct examination of fading was carried out in a similar way, but this time the cells, after staining and loading, were continuously washed with PBS without FDA. FI is therefore expected to decrease, if not by bleaching, then as a result of leakage.

To examine whether fading also contributes to the intensity decrease, a second cell tray (control) was treated identically to the first cell tray except that it was illuminated only twice, at the beginning and at the end of the experiments, 10 minutes later (solid black square). To avoid the possibility of fading during the first of the two runs, a third (control of control) cell tray was examined, in which only the last measurement was carried out. The average intensities and polarizations per cell tray obtained in these experiments are displayed in Fig. 11.

Flow Versus Static Cytometry Measurements

IFFP Measurements

Because no FC, equipped for IFFP measurements, was available, the performance comparison with the SC is based on data cited in the published literature (detailed list in Table II). When the CV was not given, the relative full-width half-maximum was calculated from the data. The results are self explanatory.

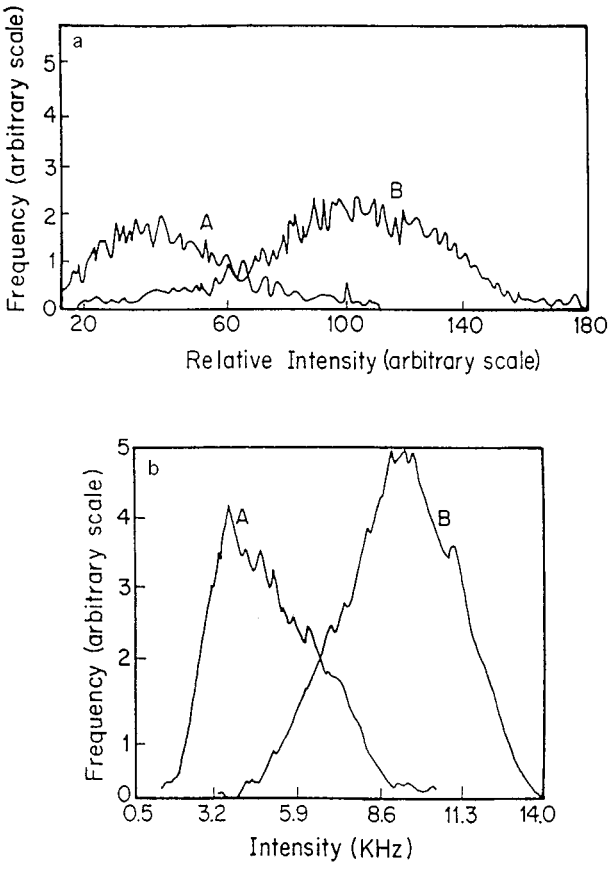

Fig. 11. FACSort flow cytometer (**a**) and ICS (**b**) performance of FI measurements on FITC-labelled human erythroleukemia line K562, incubated without (**A**) and with (**B**) FITC-labeled anti-mouse antibody.

FI Measurements

Fluorescent Beads. The same fluorescent bead suspension was repeatedly measured (10,000 events), three times by FACSort (15 mW at 488 nm, Beckton Dickinson). After each measurement the suspension was collected, concentrated by centrifuge, and resuspended. The average relative intensities, obtained in the three experiments, were correspondingly 504 $\pm$ 4, 467 $\pm$ 7, and 445 $\pm$ 8 (Fig. 12, solid circles). A control sample was treated similarly, except for laser illumination, which was applied only on the fourth run, yielding 502 $\pm$ 7 (Fig. 13, solid triangle).

The results strongly indicate that, in this test, the intensity decrease is mainly a result of photobleaching.

One hundred beads, of the same batch of beads, were illuminated for measurement during 25 scans in succession by the ICS, with no indication of any detectable photobleaching effect (data not shown).

Living Cells. FI measurements of living human erythroleukemia line K562 were performed by the FACSort and ICS cytometers. The results are presented in Fig. 13.

K562 blasts are multipotential, hematopoietic malignant cells that spontaneously differentiate into recognizable progenitors of erythrocytic, granulocytic, and monocytic series. The cells were incubated with H-9, a mouse-monoclonal antibody against human erythroid-specific antigen. This antigen is a 70-Kd membrane glycoprotein, which localized on the surface of about 100% of mammalian nucleated erythroid cells. The H-9 antibodies were visualized by FITC conjugated anti-mouse antibody.

Data from two sets of sources were obtained:

1. The control group consists of cells applied with only the FITC conjugated, anti-mouse antibody. The fluorescence of these cells should be very low because it reflects the non-specific binding of the antibodies.
2. The second source is cells treated with antibody H-9 and thereafter with FITC-labeled anti-mouse antibody. These cells should give a higher fluorescence level, which reflects the antigenic epitopes expressed on the cell surface.

The average intensity ratio between cell groups 1 and 2 was found to be 1:3 by both FACSort (I) and ICS (II). Nevertheless, the FACSort statistics are based on a sample

Table II. IFFP Parameters and Performances of Measurement in Flow and Static Cytometry

Type of cells	Mode of Separation	System/Light source	I_{ex}	λ_{ex} (nm)	$\varepsilon(\lambda_{ex})/\varepsilon(488)$	EmBW (nm)	FDA con. ($\times 0.6$ μM)	Staining Duration (min)	# of Cells measured	CV%	RFWHM%	Ref.
PHBL	LP	FC Ar laser 5 W	750 mW	488	1	LWCF > 530	400	10	30,000	16 (avg.)	68 (avg.)	[17]
PHBL	LP	FC Ar laser 5 W	1,000 mW	488	1	LWCF > 505	2	~60	>10,000		25	[18,19]
PHBL	LP	FC HeCd 10 mW	~5 mW	442	0.17	522 ± 7.5	1	30	>10,000	~71	167	[63]
NHIK	—	FC Ar 5 W	800 mW	488	1	LWCF > 525	2	3	50,000	14–20	22–35	[14]
PHBL	LP	ICS He-Cd 15 mW	$4 \cdot 10^{-3}$ mW	442	0.17	527 ± 5	0.25–1	5	180	7.5 (avg.)	15	DNS

PHBL: Peripheral human blood lymphocyte; NHIK: established human cell line NHIK-3025; LP: lymphprep; FP: Ficoll paque; λ_{ex}: excitation wavelength; ε: molar decadic absorption coefficient; EmBw: emission band width; Con: concentration; RFWHM: relative full width half maximum; LWCF: long wavelength cut-off filter; nm: nanometer; avg: average; DNS: data not shown.

size of 5,000 cells yielding a CV of 70% while that of the ICS yields a CV of 50%, based on one scanned field of 20 × 20 wells with approximately 70% (280 cells) occupancy.

By and large, cell viability and plasma membrane integrity of the measured cells was checked by restaining the same cells with propidium iodide (PI). At the end of the measurement the cells were washed twice with fresh buffer and a solution containing PI (2.5 μg/ml) was added on top of the pretested localized cells for 5 minutes. Cells were then washed twice and another measurement performed. Positive PI cells were excluded from the analysis.

DISCUSSION

It has been shown that, with FC, an illumination intensity of 4.9 W is required to obtain reasonable accuracy for the IFFP measurement (CV of 3%). The employment of such a single line (or narrowband) light source in cytometers is not realistic. Moreover, such high power might lead to effects that will change the illuminated fluorescent marker, not to mention influencing the cells themselves. However, experience shows [29,31,38,50] that such effects occur even at much lower intensities.

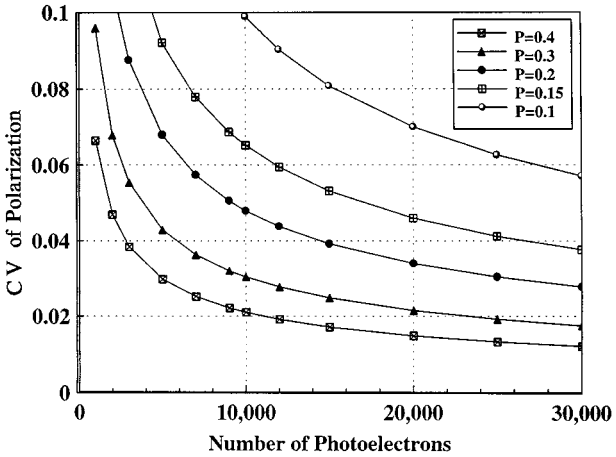

Fig. 12. Calculated CV of polarization as a function of the number of photoelectrons, for a selection of polarization P values.

Photosaturation

Photosaturation is the effect in which, beyond a certain excitation intensity, no increase in the fluorescence intensity is observed, with increasing excitation intensity (for the cases in which no structural changes in the excited molecules occur). The reason for saturation is that with increasing excitation intensity, the number of molecules in the excited state increases. Because the excited molecules are transparent to the exciting radiation, those in this state do not contribute to the fluorescence.

The intensity at which this will occur, namely the state at which the rate of excitation equals the rate of emission, depends on the absorption coefficient of the fluorescent molecules and on their decay time. Photosaturation may be an obstacle in FP measurements, particularly in viscous media.

When fluorescent markers in cells or beads are excited by polarized light, molecules whose dipole moment of absorption are parallel to the direction of the exciting field, are predominantly excited while those in other directions absorb less. When the photosaturation process takes place, at the first stage, it leads to an absorption saturation of the parallel dipoles while those at an angle to the exciting field continue to increase their emission with increasing excitation intensity. Apparently, this causes a decrease in the measured polarization. This is a possible explanation of the findings of Keene and Hodgson [28] and Pinkel *et al.* [46], which show that the

polarization of fluorescent beads decreases with increasing excitation energy.

Photobleaching

Photobleaching is the process whereby fluorescent molecules enter a state in which they are non-fluorescent. Several mechanisms can cause this to occur. One is photoisomerization, by which one of the isomeric states is nonfluorescent (a classical example is the transition from *trans*-stilbene to *cis*-stilbene). Other possible mechanisms are photodisintegration and photochemical interactions between similar or foreign molecules. Even if the primary photo product is linearly dose dependant, in many cases, the final chemical bleached product is not linearly related to the illumination power density (PD), as is the total bleaching process [51,52]. These processes depend on the structure of the molecule, on the excitation wavelength used, the temperature and presence of foreign molecules [53] (in particular, oxygen for interactions in the triplet state), and, of course, the PD of the exciting radiation. Such non-linear dependence may not be noticed when a low PD is used.

At very high excitation intensities, two photons may be involved non-linearly in the photobleaching of one molecule. One such process is double-photon excitation, that is, the simultaneous absorption of two photons (even when the molecule has no real stationary levels for the incident energy). Another is the sequential two–single-photon absorption, in which a molecule in the first excited singlet state (S_1) absorbs another photon, provided it possesses some upper level (S_n) to which such absorption may lead. Two-photon absorption has been observed only for intensities $>10^6$ W/cm^2. In flow systems, such pulse intensities might not be so rare ($\sim 5 \cdot 10^6$ W/cm^2 for a reasonable accuracy of IFFP measurement). With PD values of the order of 1–3 W/cm^2, in order to perform accurate IFFP measurements that are used in the ICS, these effects are precluded.

A very important aspect of photobleaching is its influence on the measured FP. Photobleaching was found to reduce the degree of polarization (the polarization was reported to decrease non-linearly with intensity, for high excitation intensities, particularly in viscous media [28,29]. The reason for this, it is believed, might be the higher rate of photobleaching of those molecules, having their absorbtion dipole moment parallel to the polarized excitation electric field, than of those subtending an angle δ with it. In fact, the latter are illuminated by a PD that is lower by a factor of $\cos^2\delta$. This effect yields a decrease in FP. It may, however, also lead to an increase in the degree of polarization. For example, the degree of FP of cells that were colored with diphenyl hexatriene (DPH), has been shown to increase with time when these cells are attached to a quartz plate (but not when they were free to move in a liquid suspension) [54]. The reason for this is that in the fixed cells, in those DPH molecules at a site where they could freely rotate, isomerization could take place, whereas those more rigidly caged could isomerize less, and continued to emit their fluorescence, which, because of the rigidity of the cage, was more strongly polarized.

Furthermore, in the case of intensity measurements, the collecting detector measures $I_M = I_\parallel + I_\perp$ and not the total intensity $I_T = I_\parallel + 2I_\perp$. It is readily shown that $I_M/I_T = 2/3 - P$, where P is the emitted FP. Therefore when photosaturation and/or photobleaching cause changes in the true FP, they also directly impair the intensity measurements. This argument can also be shown to hold when the excitation beam (normal to the detection direction) is natural-polarized (unpolarized). Therefore, if accurate FI measurements are desired (particularly if they are not linearly dependent on the excitation intensity), $I_T = I_\parallel + 2I_\perp$ should be measured while horizontally polarized excitation is employed. Alternatively, using *magic* angles, which cancel the dependence of FI on FP, is also an option. It should be emphasized here that in many cases photobleached FP is desired. One such case is the examination of molecular rotational diffusion [55,56].

The situation with the ICS is quite different and is attributed to the fact that the power that reaches the cell is 5–6 orders of magnitude less than the average power used in FC. When stepwise increasing the output of the laser from 50–200 mW, the overall FI emitted from fluorescent beads (given by $I_\parallel + 2I_\perp$), increases linearly with the laser output (see Fig. 7). The results in Figs. 8 and 9 show the same tendency. This is different from the results obtained using FC [28,29,36,46], where photobleaching effects were found to occur in outputs above 5 mW.

Fading also was not noticeable in experiments with individual living cells, after 10 exposures, during which FI and FP were measured (see Fig. 10). It was previously shown [50] that the dynamic process of cell staining by fluorescein can be described satisfactorily by the rate equation:

$$\frac{dF_{ic}}{dt} = \alpha F_A - \beta F_{ic}$$

where F_{ic} is intracellular (ic) fluorescein concentration, F_A is the FDA concentration in the solvent, α is the rate constant for F_{ic} formation, and β is the rate constant of F_{ic} leaking out of the lymphocytes.

Under the assumption that $F_{ic} = 0$ for $t = 0$, one obtains:

$$F_{ic}(t) = \frac{\alpha}{\beta} F_A(1 - e^{-\beta t})$$

After about 6 minutes, cell staining reaches a steady state where $F_{ic}(t)$ saturates approximately at the constant theoretical value of $\frac{\alpha}{\beta} F_A$.

In the experiment shown in Fig. 10, the cellular fluorescein efflux was continuously washed away with staining solution, keeping the cells in their steady-state phase of staining. Thus, if no fading occurs, the measured FI values should be constant. If, however, fading took place, the FI should continuously decrease. Indeed, after 10 repeated excitation exposures of typically 100 ms each, the measured FI remains constant: FI = 74.14 ± 0.68 KHz (CV = 0.92%) (see Fig. 10), indicating that if fading took place at all, it was not notable.

Direct examination of fading was carried out (see Fig. 11) and indicated no notable fading. By contrast, comparison with experiments of repeated FI measurements performed by FACSort (15 mW output) indicated a notable bleaching effect (see Fig. 12). The excellent repeatability demonstrated in Fig. 10, together with the results presented in Fig. 11 (which indicate that the decrease in the FI of the illuminated sample is similar to that obtained with the control irradiated cell trays by dye efflux) suggest that the appropriate SC system might have no measurable effect on the measured sample.

The fact that fading is absent or negligible under these working conditions cannot be attributed to a poor signal-to-noise ratio of the ICS, especially in light of the calculations, experiments, and discussion presented in this study. Moreover, this is in agreement with the commonly accepted opinion that SC cytometers provide greater sensitivity than flow cytometers [45].

The subject of photobleaching seems to be controversial. Some authors [26,28,46] claim that photobleaching occurs at illumination levels as low as 5 mW, whereas others [29] state that photobleaching or fluorescence saturation may become important only when excitation levels exceed 100 mW.

Immunoassay FI experiments of comparative measurements were conducted by FACSort and SC on human erythroleukemia line K562 (see Fig. 13). The intensity ratio between FITC-labeled cells, incubated without (control), and antibody H-9 was found to be 1:3 both by the FACSort and the SC. Despite the fact that FACSort statistics were based on a sample size of 5,000 cells, whereas those of the SC were based on only 280 cells, CV values were 70% and 50%, respectively.

This result is in agreement with the fact that although low-power lasers have been used extensively for light scatter measurements in flow cytometers [57], their use for immunofluorescence measurements is less common.

Photodamage to Cells by Light in the Visible Region

The present study deals with the correct conditions of applying FP measurements as a cellular functional parameter, therefore photodamage or photobiostimulation might distort the true results.

Sheetz and Koppel [53] investigated the membrane damage induced on FITC-labeled concanavalin A (F-con A)-labeled erythrocyte ghost suspensions by 488-nm illumination at intensities of up to 450 W/cm^2. They reported protein aggregation on SDS-PAGE gels. They further noted that photodamage was nonlinearly related to the total incident beam power.

Shapiro (Shapiro, 1983 Patent) used a laser beam of 10 W to kill acute lymphoblastic leukemia cells in a suspension flowing in a thin stream of 50–200 μm diameter at a velocity of 20 m/s. They were exposed to an illumination pulse of an argon laser of roughly 10-μsec duration. The size of the light spot in the focal plane had to be 300 μm. Assume, for calculation simplification, that the beam PD is homogeneous. The PD at the illuminated area is therefore:

$$PD = \frac{10\ W}{\pi(150)^2\ \mu^2} = 1.42 \cdot 10^4 \frac{W}{cm^2}$$

This intensity is 4 orders of magnitude greater than that used in the ICS and approximately 2 orders of magnitude smaller than the PD necessary for a proper IFFP measurement with FC. Two mechanisms, which induce photolysis at differing rates, were suggested by Bloom and Webb [51]: (1) local thermal shocks exceeding ~5°C; and (2) massive contraction of the membrane cytoskeleton. Mechanism 1 proceeds rapidly and is avoided by maintaining incident laser intensities well below 1 mW. Mechanism 2 is chromophore stimulated, but its rate is highly dependent upon the oxygen concentration in the buffer. Upon oxygen removal, at low beam intensities, mechanism 2 yields simple linear dose kinetics.

The fact that the increase of temperature depends on the relation between the rate of heat supply and heat dissipation is trivial. Thus temperature increase is much more sensitive to PD than to illumination dose.

Photobiostimulation

Biostimulatory effects of low-output laser irradiation have been demonstrated at various molecular and cellular

levels, as well as at whole organ and tissue levels. Under certain circumstances, synergistic effects with laser irradiation have been found as demonstrated in the immune system [58–61]. Existing evidence shows that effects can occur far from the irradiated site, suggesting the presence of a circulatory active substance. With sufficient intensity, the stimulatory effect disappears and inhibition occurs. Most of the experiments show that low-energy lasers do have specific bioeffects, which seem to change from stimulatory to damaging, with increasing doses. Moreover, bioeffects were found to be not only dose dependent but also non-linearly intensity-dependent [52].

In general, non-linearity in photo-induced changes is defined as a process in which linear optical absorption produces active chemicals (such as cytoplasmic H^+ and Ca^{2+}), which participate in chemical reactions, whose reaction rates are non-linearly dependent on the concentration of these photo-produced active chemicals. The results are thus a non-linear function of the illumination intensity.

Such phenomena most probably affect functional parameters such as IFFP, where the physiological status of the cell is investigated. The measuring technique and conditions might induce biological processes in the measured sample, thereby affecting the measurement. This article tries to investigate the parameters that influence the proper outcome of IFFP measurements. Scientific, and clinical results, which depend on the proper execution of these measurements, are many, some of which have been briefly mentioned in the introduction above.

APPENDIX A: THE DEPENDENCE OF FP ON THE NUMERICAL APERTURE (NA)

The measurement of FP (also termed *P,* for brevity), calls for the summation of all FI (also termed *I* for brevity) emitted into the solid angle defined by the aperture of the measuring system. This solid angle is defined by Φ and Θ, which are the limits, respectively, of ϕ and θ, shown in Fig. 2, namely:

$$I_\perp(\Theta, \Phi) = \sum i_\perp(\theta, \phi),\ I_\parallel(\Theta, \Phi) = \sum i_\parallel(\theta, \phi)$$

The measured value of the polarization is:

$$P(\Theta, \Phi) = \frac{\sum i_\parallel(\theta, \phi) - \sum i_\perp(\theta, \phi)}{\sum i_\parallel(\theta, \phi) + \sum i_\perp(\theta, \phi)}$$

or

$$P(\Theta, \Phi) = \frac{\int_0^\Phi \int_0^\Theta (i_\parallel - i_\perp)\, d\theta\, d\phi}{\int_0^\Phi \int_0^\Theta (i_\parallel + i_\perp)\, d\theta\, d\phi}$$

In Fig. 2 we see the relationship between the intensities in the various directions:

$$i_\parallel \equiv i_z = I_z \cos^2\theta + I_x \sin^2\phi \sin^2\theta + I_y \cos^2\phi \sin^2\theta \quad \text{(A1)}$$

$$i_\perp = i_x = I_x \cos^2\phi + I_y \sin^2\phi \quad \text{(A2)}$$

From symmetry considerations, $I_x = I_y = I_\perp$ and $I_z = I_\parallel$. From equations (A1) and (A2) the result is:

$$i_\parallel = I_\parallel \cos^2\theta + I_\perp \sin^2\theta$$

$$i_\parallel = I_\perp$$

Integration of $P(\Theta, \Phi)$ over ϕ yields a factor Φ in both the numerator and denominator, thus:

$$P(\Theta, \Phi) = \frac{\int_0^\Theta [(I_\parallel \cos^2\theta + I_\perp \sin^2\theta) - I_\perp]\, d\theta}{\int_0^\Theta [(I_\parallel \cos^2\theta + I_\perp \sin^2\theta) + I_\perp]\, d\theta}$$

$$= \frac{\int_0^\Theta [(I_\parallel - I_\perp)\cos^2\theta]\, d\theta}{\int_0^\Theta [(I_\parallel - I_\perp)\cos^2\theta]\, d\theta + \int_0^\Theta 2I_\perp\, d\theta}$$

$$= P(\Theta) \quad \text{(A3)}$$

The reciprocal of $P(\Theta)$ gives:

$$\frac{1}{P(\Theta)} = 1 + \frac{2I_\perp}{I_\parallel - I_\perp} \cdot \frac{\int_0^\Theta d\theta}{\int_0^\Theta \cos^2\theta\, d\theta}$$

$$= 1 + \frac{1 - P}{P} \cdot \frac{2\Theta}{\Theta + \frac{1}{2}\sin 2\Theta}$$

$$= 1 + \frac{2(1 - P)}{P\left(1 + \frac{\sin 2\Theta}{2\Theta}\right)} \tag{A4}$$

where $\frac{2I_\perp}{I_\parallel - I_\perp} \cdot = \frac{2P}{(1 - P)}$

The envelope of the collected light beams is symmetrical with regard to the optical axis of the measuring system and, hence, $2\theta = 2\phi \equiv X$. Therefore,

$$\frac{1}{P(X)} = 1 + \frac{2(1 - P)}{P\left(1 + \frac{\sin X}{X}\right)}$$

$$= \frac{P\left(1 + \frac{\sin X}{X}\right) + 2 - 2P}{P\left(1 + \frac{\sin X}{X}\right)}$$

$$= \frac{2 - P\left(1 - \frac{\sin X}{X}\right)}{P\left(1 + \frac{\sin X}{X}\right)} \tag{A5}$$

and finally:

$$\frac{1}{P(X)} = \frac{2}{P\left(1 + \frac{\sin X}{X}\right)} - \frac{\left(1 - \frac{\sin X}{X}\right)}{\left(1 + \frac{\sin X}{X}\right)} \tag{A6}$$

The common numerical aperture of a microscope's objective for routine use (NA $\cong$ 0.25) gives X $\cong$ 30°. In this case, the contribution of the second component on the right side of the equation is less than 1% of the measured polarization P(x) for P = 0.200 and can thus be neglected in most cases (in the SC, where X = 74° it is less than 3%). The approximate value of P(X) for small X, is given by P*(X):

$$\frac{1}{P^*(X)} = \frac{2}{P\left(1 + \frac{\sin X}{X}\right)} \tag{A7}$$

As the aperture angle X decreases to 0 (i.e., the system changes from microscopic to macroscopic), the polarization becomes independent of the angle and P(X) reduces to P.

APPENDIX B: CALCULATION OF FP COEFFICIENT OF VARIANCE (CV)

To avoid excessive subscripts, $I_\parallel \equiv A$ and $I_\perp \equiv B$ is defined. The degree of polarization is then defined by $P = \frac{A - B}{A + P}$. Thus:

$$dP = \frac{\partial P}{\partial A}\,dA + \frac{\partial P}{\partial B}\,dB$$

$$= \left[\frac{(A + B) - (A - B)}{(A + B)^2}\right] dA$$

$$+ \left[\frac{-(A + B) - (A - B)}{(A + B)^2}\right] dB$$

$$= \frac{2B}{(A + B)^2}\,dA + \frac{-2A}{(A + B)^2}\,dB$$

gives the contribution of error from A and from B. For interest in the maximum error, the absolute values of the contributions are added:

$$dP = \frac{2B}{(A + B)^2}\,dA + \frac{2A}{(A + B)^2}\,dB$$

$$= \frac{2A \cdot B}{(A + B)^2}\left(\frac{dA}{A} + \frac{dB}{B}\right)$$

But $2AB = 1/2\,[(A + B)^2 - (A - B)^2]$. Therefore:

$$dP = \frac{1 - P^2}{2}\left(\frac{dA}{A} + \frac{dB}{B}\right).$$

The relative error dP/P is CV

$$\frac{dP}{P} = \frac{1 - P^2}{2P}\left[\frac{dA}{A} + \frac{dB}{B}\right].$$

Assume:

$$\frac{dA}{A} \approx \frac{dB}{B}$$

provided the values of A and B are in the same range. Then:

$$\frac{dA}{A} + \frac{dB}{B} \approx \frac{2dA}{A} = \frac{2\sqrt{N_{pe}}}{N_{pe}} = \frac{2}{\sqrt{N_{pe}}}$$

where N_{pe} is the number of photoelectrons. The CV is then

$$\frac{dP}{P} = \left(\frac{1 - P^2}{P}\right)\frac{1}{\sqrt{N_{pe}}}$$

This relationship is shown in Fig. 14, which gives the

CV of the polarizations as a function of the number of photoelectrons, for a selection of polarization P values. Hence,

$$N_{pe} = \left[\left(\frac{1 - P^2}{P}\right) 1 \Big/ \frac{dP}{P}\right]^2 \qquad \text{(B1)}$$

N_{pe} can be predetermined by the preset count arrangement of the ICS, enabling the predetermination of the accuracy of the measurements and the resulting CV, which can be set to be identical for all cells, independent of their intensities. Thus the minimum value of photoelectrons needed for a given CV is obtained. For example, for a value of P of about 0.2, and an error not exceeding 1%, for the polarization measurement of a single cell, the number of photoelectrons needed is given by:

$$\frac{dP}{P} = 10^{-2} = \frac{1 - (0.2)^2}{0.2} \cdot \frac{1}{\sqrt{N_{pe}}}$$

Hence:

$$N_{pe} = \left[\left(\frac{1 - (0.2)^2}{0.2}\right) \cdot 10^2\right]^2 = 230{,}000$$

For a CV of 3% the number of required photoelectrons is:

$$N_{pe}(3\%) = \left(\frac{1 - (0.2)^2}{0.2} \cdot \frac{100}{3}\right)^2 = 25{,}600$$

For a CV of 3% and a polarization of 0.3, the number of required photoelectrons is 10,223. For a CV of 3% and a polarization of 0.15, the number of required photoelectrons is 47,186.

APPENDIX C: CALCULATION OF THE ABSORPTION OF THE INCIDENT RADIATION BY A STAINED LYMPHOCYTE

A lymphocyte is a spherical cell. Therefore the length of the optical path of the incident radiation within the cell depends on the distance of the path from the center of the sphere. The overall absorption is obtained by summation over all possible optical path lengths. The intensity cross section of the exciting beam is assumed to be Gaussian. The incident radiation is divided into cylindrical layers of light of a cross section area "ds" each. The intensity of the radiation that enters such a cylindrical shell is $i(r) \cdot ds = i_0 \exp(-2r^2/\omega^2)\, ds$, where $i(r)$ is the PD. The absorption along each path, a(r), obeys the Beer-Lambert law. Because the loss of intensity as a result of absorption by the cells is very small, the following can be approximated:

$$\begin{aligned} a(r) &= i(r)(1 - e^{-2.3\varepsilon c l(r)})\, ds \\ &\cong i(r)2.3\varepsilon c l(r)\, ds \\ &= i(r)2.3\varepsilon c dV \end{aligned} \qquad \text{(C1)}$$

where ε is the molar decadic absorption coefficient, c the concentration of fluorescein, and r the radius of a cylindrical shell of thickness dr, which absorbs light along $l(r)$, the cylinder path length. It is easily seen that $r = R \sin\theta$, and $dr = R \cos\theta\, d\theta$, where R is the radius of the cell.

The area of the cross section of the cylindrical shell is $ds = 2\pi r\, dr = 2\pi R \sin\theta\, dr$. The volume dV of the shell is $2\pi\, dr\, l(r)$, where $l(r) = 2R \cos\theta$.

Hence:

$$\begin{aligned} dV &= ds \cdot l(r) = 2\pi r\, dr\, l(r) \\ &= 2\pi R \sin\theta\, dr \cdot 2R \cos\theta \\ &= 2\pi R \sin\theta \cdot R \cos\theta\, d\theta \cdot 2R \cos\theta \\ &= 4\pi R^3 \cos^2\theta \sin\theta\, d\theta \end{aligned}$$

The amount of absorbed radiation will be:

$$A = \int a(r)\, dV$$

$$= \int_0^{\pi/2} i(r) \cdot 2.3 \cdot \varepsilon \cdot c \cdot 4\pi R^3 \cos^2\theta \sin\theta\, d\theta =$$

$$A = -4\pi R^3\, 2.3\varepsilon c \int_1^0 i_0\, e^{-2r^2/\omega^2} \cos^2\theta\, d(\cos\theta)$$

In this calculation the cell is assumed to be homogenously stained and placed so that its center coincides with that of the laser beam while its surface touches the Gaussian intensity envelop at the distance ω from the beam center.

Define $4\pi R^3(2.3)\varepsilon c i_0 \equiv K$, and since $r = R \sin\theta$:

$$A = -K \int_1^0 e^{-(2R^2 \sin^2\theta)/\omega^2} \cos^2\theta\, d(\cos\theta)$$

$$= -K \int_1^0 e^{-2R^2(1-\cos^2\theta)/\omega^2} \cos^2\theta\, d(\cos\theta) =$$

$$= -K e^{-2R^2/\omega^2} \int_1^0 e^{-2R^2 \cos^2/\omega^2} \cos^2\theta\, d(\cos\theta)$$

Defining $\cos\theta = X$, $d(\cos\theta) = dX$ yields:

$$A = -Ke^{-2R^2/\omega^2} \int_1^0 e^{-2R^2X^2/\omega^2} X^2 dX$$

Multiplying and dividing by $4\omega^2/R^2$:

$$A = \left(\frac{4R^2}{\omega^2}\right)^{-1} \cdot \left(-Ke^{\frac{-2R^2}{\omega^2}}\right) \int_1^0 X \left(\frac{4R^2}{\omega^2} Xe^{-\frac{2R^2}{\omega^2}X^2}\right) dX$$

and integrating by parts, yields:

$$A = \left(\frac{4R^2}{\omega^2}\right)^{-1} \left(-Ke^{-\frac{2R^2}{\omega^2}}\right) \left[Xe^{-\frac{2R^2}{\omega^2}X^2}\Big|_1^0 - \int_1^0 e^{-\frac{2R^2}{\omega^2}X^2} dx\right]$$

The integral on the right is of the form $\exp(2aX^2)\ dX$ and can be solved numerically, provided that the ratio R^2/ω^2 is defined. In our case, $\omega = R$, which means that the intensity of this shell beam that excites the outermost parts of the cell equals i_0/e^2.

$$A = -\frac{1}{4} Ke^{-2} \left[Xe^{2X^2}\Big|_1^0 - \int_1^0 e^{2X^2} dX\right]$$

$$= -\frac{1}{4} Ke^{-2} \left[-e^2 - \int_1^0 e^{2X^2} dX\right] =$$

$$= \frac{1}{4} K \left(1 + e^{-2} \int_1^0 e^{2X^2} dX\right)$$

Inserting the expression for K, yields:

$$\frac{1}{4} 4\pi R^3\ 2.3\varepsilon c i_0 \left(1 + e^{-2} \int_1^0 e^{2X^2} dX\right) \qquad (C2)$$

The intensity i_0 of the beam at $r = 0$ is unknown. However, its expression in terms of I_0 (the overall intensity of the beam) is known, namely:

$$I_0 = \int_0^\infty i_0 e^{-\frac{2r^2}{\omega^2}} 2\pi r\ dr = \pi i_0 \int_0^\infty e^{-\frac{2r^2}{\omega^2}} 2r\ dr$$

Changing the variable r^2 into x, then $dx = 2r\ dr$ and:

$$I_0 = \pi i_0 \int_0^\infty e^{-\frac{2r^2}{\omega^2}} dx = \pi i_0 \frac{-\omega^2}{2} e^{-\frac{2r^2}{\omega^2}}\Big|_0^\infty$$

$$= -\pi i_0 \frac{-\omega^2}{2} (-1) = \frac{\pi\omega^2 i_0}{2}$$

The result shows that the overall intensity of the beam equals the cross-sectional area of the beam, times half of the maximum intensity (the intensity of the central part of the beam), therefore:

$$i_0 = \frac{2I_0}{\pi\omega^2} \qquad (C3)$$

Insertion of Eq. (C3) into Eq. (C2) yields:

$$A = \pi R^3\ 2.3\varepsilon c \frac{2I_0}{\pi\omega^2} \left(1 + e^{-2} \int_1^0 e^{2X^2} dX\right) \qquad (C4)$$

Inserting $\omega = R$ into eq. (C4) yields:

$$A = I_0\ 2.3\varepsilon c(2R) \left(1 + e^{-2} \int_1^0 e^{2X^2} dX\right) \qquad (C5)$$

The numerical evaluation of the integral in Eq. (C5) yields -2.3, finally, giving for A

$$A = I_0\ 2.3\varepsilon c(2R)0.68.$$

Suitable consideration should be made when integrating a(r) over the cell volume, in a case in which the cell is heterogeneously stained, say subcellular fractions that are specifically stained or cells stained with different dyes having different absorption coeffiecients. In that case, the integration constants, ε and *c*, should be replaced by $\varepsilon(r, \theta, \phi)$ and $c(r, \theta, \phi)$. In a case in which the beam and the cell centers do not coincide, a phenomena that frequently exists in FC and laser scanning microscopy (LSM), the emitted intensity profile from the cell (even when homogeneously stained) will be the convolution outcome of the laser intensity cross section i(r) and the multiplication εc, a fact that might influence measurements of cell size distribution when assesed by their FI, as well as cell images when using LSM. The latter is usually, but unfortunately not successfully, corrected via deconvolution [62].

APPENDIX D: CALCULATION OF THE FLOURESCEIN CONCENTRATION IN LYMPHOCYTES

Repeated classical IFFP measurements using cuvette showed that the bulk concentration of fluorescein in the

cell suspension changes during a FP measurement from 10^{-10}–10^{-9} M. For calculation purposes, an average concentration of fluorescein of 5×10^{-10} M is chosen. A comparison of the FI of the cell suspension with that of the suspending liquid alone, shows that about $\frac{2}{3}$ of the signal comes from the cells, assuming the quantum yield of fluorescein in the cells to be equal to that in solution. It can thus be stated that about $\frac{2}{3}$ of the fluorescein is within the cells. The overall concentration of fluorescein within the whole ensemble of cells is therefore $\frac{2}{3} \times 5 \cdot 10^{-10}$ M. The suspension of cells for the measurement is achieved by mixing of 0.2 ml of cell suspension of 6×10^6 cells/ml with 3 ml of PBS + FDA. The overall volume of the measured cell suspension is thus 3.2 ml and contains $0.2 \times 6 \times 10^6 = 1.2 \times 10^6$ cells. The volume of one lymphocyte of 7 μm diameter is

$$\frac{4\pi}{3}(3.5 \cdot 10^{-4}\ \text{cm})^3 = 0.18 \cdot 10^{-12}\ \text{liter}$$

Assuming the average concentration of fluorescein in a single cell, within the whole population of cells to be homogeneous, the average concentration of fluorescein within the cells is found to be

$$\frac{\text{quantity of fluorescein (in moles) in the cells of one liter of cell suspension}}{\text{volume of cells in one liter of cell suspension}}$$

$$= \frac{\frac{2}{3} \cdot 5 \cdot 10^{-10}\ \text{mole}}{1.2 \cdot 10^6 \left(\frac{1000\ \text{ml}}{3.2\ \text{ml}}\right) \cdot 0.18 \cdot 10^{-12}\ \text{liter}} = 5 \cdot 10^{-6}\ \text{M}$$

APPENDIX E: CALCULATION OF THE INTENSITY OF THE GAUSSIAN LASER BEAM PASSING THE PINHOLE

The intensity of the Gaussian laser beam passing the pinhole (I_{ph}) of diameter 2k is given by:

$$I_{ph} = 2\pi \int_0^k i_0\, e^{-\frac{2r^2}{\omega^2}}\, r\, dr = i_0\, \pi \int_0^k e^{-\frac{2r^2}{\omega^2}}\, 2r\, dr \quad \text{(E1)}$$

Defining $r^2 = X$, $dx = 2r\, dr$ for $r = 0$, $X = 0$; for $r = k$, $X = k^2$, Eq. (E1) yields:

$$i_0\pi \int_0^{k^2} e^{-\frac{2r^2}{\omega^2}}\, dx = \frac{i_0}{2}\, \pi\omega^2 \left(1 - e^{-\frac{2r^2}{\omega^2}}\right) \quad \text{(E2)}$$

The magnitude of i_0 as expressed by I_0, the output intensity of the laser (see Eq. [C3] Appendix C) is $i_0 = 2I_0/\pi\omega^2$. Introducing this value into Eq. (E2) gives:

$$I_{ph} = I_0 \left(1 - e^{-\frac{2k^2}{\omega^2}}\right)$$

Hence,

$$k = \omega \sqrt{\ln\left(1 - \frac{I_{ph}}{I_0}\right)^{-\frac{1}{2}}}$$

Since $I_{ph}/I_0 << 1$, the approximate result is:

$$k = \omega \left[\ln\left(1 + \frac{1}{2}\frac{I_{ph}}{I_0}\right)\right]^{\frac{1}{2}}$$

The output intensity of the He-Cd laser used in the SC is ≅ 10 mW, and ω ≅ 1 mm (=1,000 μm). Therefore, for a requested intensity $I_{ph} = 3 \cdot 10^{-6}$ W:

$$k = 1{,}000\ \mu\text{m} \left[\ln\left(1 + \frac{1}{2} \cdot \frac{3 \cdot 10^{-6}}{10^{-2}}\right)\right]^{\frac{1}{2}} = 12.25\ \mu\text{m}$$

or the diameter of the pinhole must be 25 μm.

REFERENCES

1. H. M. Shapiro (1995) in Wiley-Liss (Ed.) *Practical Flow Cytometry,* 3rd ed, John Wiley and Sons, New York.
2. J. Alberola-Ila, S. Takaki, J. D. Kerner, and R. M. Perlmutter (1997) *Annu. Rev. Immunol.* **15**, 125–154.
3. A. Weiss (1993) in W. E. Paul (Ed.) *Fundamental Immunology,* 3rd ed, Raven Press Ltd., New York, pp. 467–504.
4. M. Van Graft, Y. M. Kraan, I. M. Segers, K. Radosevic, B. G. De Grooth, and J. Greve (1993) *Cytometry,* **14**, 257–264.
5. A. Ben-Ze'ev, and A. D. Bershadsky (1997) *Adv. Mol. Cell. Biol.* **24**, 125–163.
6. G. Berke (1993) in W. E. Paul (Ed.) *Fundamental Immunology,* 3rd Edition, Raven Press Ltd., New York, pp. 965–1014.
7. B. Geiger, D. Rosen, and G. Berke (1982) *J. Cell. Biol.* **95**, 137–143.
8. L. Cercek and B. Cercek (1977) *Europ. J. Cancer* **13**, 903–915.
9. M. Sunray, M. Kaufman, N. Zurgil, and M. Deutsch (1999) *Biochem. Biophys. Res. Commun.* **261**, 712–719.
10. M. Kaplan, E. Trebnyikov, and G. Berke (1997) *J. Immunol. Methods* **201**, 15–24.
11. N. Zurgil, Y. Levy, B. Gilburd, E. Trubiankov, M. Deutsch, Y. Shafran, Y. Shoenfeld (2001) in Y. Shoenfeld and D. Harats, G. Wick (Eds.) *Atherosclerosis and Autoimmunity,* Elsevier, New York, pp. 191–200.
12. B. J. Atkinson, W. S. Lowry, P. Strain (1983) *Cancer* **52**, 91–100.
13. K. D. Bagshawe (1977) *Br. J. Cancer* **35**, 701.

14. L. Cercek, B. Cercek, and C. I. V. Franklin (1974) *Br. J. Cancer* **29**, 345–352.
15. J. P. Dickinson, J. E. D. Dyson, J. J. Smith, and N. Cowley (1976) in M. Dekker (Ed.) *Proc. 3rd Int. Congr. Soc. Detect. Prev. Cancer*, New York.
16. G. R. Hockling, J. M. Rolland, R. C. Nairn, E. Phil, A. M. Cuthbertson, E. S. R. Hughes, and W. R. Johnson (1982) *J.N.C.I.* **68**(4), 579–583.
17. H. Mitchell, O. Wood, C. R. Pentycross, E. Abel, and K. D. Bagshawe (1980) *Br. J. Cancer* **41**, 772–777.
18. H. Orjsaeter, G. Hordfalb, and I. Svendsen (1979) *Br. J. Cancer* **40**, 628–633.
19. A. W. Preece, P. A. Light, and P. Balding (1980) *Br. J. Cancer* **41**, 73–85.
20. J. A. V. Pritchard, W. J. Sutherland, J. E. Siddall, A. J. Bater, I. J. Kerby, T. J. Deeley, G. Griffity, R. Sinclair, B. H. Davies, A. Rimmer, and D. J. T. Webster (1982) *Eur. J. Cancer Clin. Oncol.* **18**(7), 651–659.
21. N. D. Schnuda (1980) *Cancer* **46**, 1164–1173.
22. M. Tsuda, H. Maeda, and S. Kiskimoto (1981) *Br. J. Cancer* **43**, 793–803.
23. K. Dimitropoulos, J. M. Rolland, R. C. Nairn (1986) *Biochem. Biophys. Res. Comm.* **136**, 1021–1029.
24. W. G. Eisert, W. Beisker, W. Hartmann, and R. M. Eisert (1980) *Flow Cytometry* **IV** 34–40.
25. M. Epstein, A. Norman, D. Pinkel, and R. Udkoff (1977) *J. Histochem. Cytochem.* **25**, 821–826.
26. W. Hartmann, W. Beisker, R. Eisert, and W. G. Eisert (1980a) *Flow Cytometry* **IV**, 183–186.
27. W. Hartmann, E. Sackmann, W. G. Eisert, R. Eisert, and T. M. Fliedner (1980b) *Biomedicine* **32**, 185–188.
28. J. P. Keene and B. W. Hodgson (1980) *Cytometry* **1**(2), 118–126.
29. T. Lindmo and H. B. Steen (1977) *Biophys. J.* **18**, 173–187.
30. D. Pinkel, P. Dean, S. Lake, D. Peters, M. Mendelsohn, J. Gray, M. Van Dilla, and B. Gledhill (1979) *J. Histochem. Cytochem.* **27**, 353–358.
31. G. B. Price, M. J. McCutcheon, W. B. Taylor, and R. G. Miller (1977) *J. Histochem. Cytochem.* **25**, 597–600.
32. J. M. Rolland, K. Dimitropoulos, A. Bishop, G. R. Hocking, and R. C. Nairn (1985) *J. Immunol. Methods* **76**, 1–10.
33. S. Stewart, K. I. Pritchard, J. W. Meakin, and G. B. Price (1979) *Clin. Immunol. Immunopathol.* **13**, 171–181.
34. R. Udkoff and A. Norman (1979) *J. Histochem. Cytochem.* **27**, 49–55.
35. R. Udkoff, S. Chan, and A. Norman (1981) *Cytometry* **1**, 265–271.
36. E. Ger van Den and C. Farmer (1992) *Cytometry* **13**, 669–677.
37. D. Axelrod (1989) *Methods Cell Biol.* **30**, 333–352.
38. B. Rotman and B. W. Papermaster (1966) *Proc. Natl. Acad. Sci.* **55**, 134–141.
39. E. Gelman-Zhornitsky, M. Deutsch, R. Tirosh, Y. Yistzhak, A. Weinreb, and H. M. Shapiro (1997) *J. Biomed. Opt.* **2** 186–194.
40. J. M. Rolland, R. C. Nairn, A. P. Nind, and E. Pihl (1984) *N. J. C. I.* **72**(2), 267–273.
41. W. Beisker and W. G. Eisert (1981) *Anal. Quant. Cytol.* **3**(4), 315–322.
42. W. Beisker, W. G. Eisert (1985) *Biophys. J.* **47**, 607–612.
43. W. Beisker, W. G. Eisert (1989) *J. Histochem. Cytochem.* **37**(11), 1699–1704.
44. M. Sernetz (1973) in Springer-Verlag (Ed.) *Fluorescence Techniques in Cell Biology*, Berlin-Heidelberg-New York, pp. 244–254.
45. D. Burger and R. Gershman (1988) *Cytometry* **9**, 101–110.
46. D. Pinkel, M. Epstein, R. Udkoff, A. Norman (1978) *Rev. Sci. Instrum.* **49**(7), 905–912.
47. J. P. Kratohvil, M-P. Lee, and M. Kerker (1978) *App. Optics* **17**, 1978–1980.
48. E-H. Lee, R. E. Benner, J. B. Fenn, and R. K. Chang (1978) *App. Optics* **17**, 1980–1982.
49. A. Eisenthal, O. Marder, D. Dotan, S. Baron, B. Lifschitz-Mercer, S. Chaitchik, R. Tirosh, A. Weinreb, and M. Deutsch (1996a) *Biol. Cell* **86**, 145–150.
50. M. Sunray, M. Deutsch, M. Kaufman, R. Tirosh, A. Weinreb, and H. Rachmani (1997) *Spectrochim. Acta A Mol. Biomol. Spectrosc.* **53**, 1645–1653.
51. J. A. Bloom and W. W. Webb (1984) *J. Histochem. Cytochem.* **32**(6), 608–616.
52. R. Lubart, H. Friedmann, I. Peled, and N. Grossman (1993) *Laser Therapy* **5**, 55–57.
53. M. P. Sheetz and D. E. Koppel (1979) *Proc. Natl. Acad. Sci. USA* **76**, 3314.
54. G. Duportail and A. Weinreb (1983) *Biochim. Biophys. Acta* **736**, 171–177.
55. M. Velez and D. Axelrod (1988) *Biophys. J.* **53**(4), 575–591.
56. R. Zidovetzki, Y. Yarden, J. Schlessinger, and T. M. Jovin (1981) *Proc. Natl. Acad. Sci. USA* **78**(11), 6981–6985.
57. D. Peebles, S. Kirchanski, M. Brown, and R. Hoffman (1986) *Ann. N.Y. Acad. Sci.* **468**, 104–112.
58. E. Mester, A. F. Mester, and A. Mester (1985) *Lasers Surg. Med.* **5**, 31–39.
59. N. Grossman, N. Schneid, H. Reuveni, S. Halevy, and R. Lubart (2000) *Lasers in the Life Sciences* **9**(2), 111–126.
60. R. Lubart and H. Breitbart (invited review) (2000) *Drug Dev. Res.* **50**, 471–475.
61. D. Oren, R. Lavie, D. S. Charney, and R. Lubart (2001) *Biol. Psychiatry* **5**, 464–467.
62. L. A. Kamentsky, D. Burger, R. Gershman, L. D. Kamentsky, and E. Luther (1997) *Acta Cytol.* **41**, 123–143.
63. H. Rachmani, M. Deutsch, I. Ron, S. Gerbat, R. Tirosh, A. Weinreb, S. Chaitchuk, and S. Lalchuk (1996) *Eur. J. Cancer* **23A**, 1748–1765.